Received: 2 August 2021 | Revised: 21 November 2021 | Accepted: 29 December 2021

DOI: 10.1002/jev2.12186

RESEARCH ARTICLE

Highly-metastatic colorectal cancer cell released miR-181a-5p-rich extracellular vesicles promote liver metastasis by activating hepatic stellate cells and remodelling the tumour microenvironment

Senlin Zhao[1,2] | **Yushuai Mi**[3] | **Binbin Zheng**[4] | **Ping Wei**[2,5,6] | **Yanzi Gu**[7] | **Zhengxiang Zhang**[8] | **Ye Xu**[1,2] | **Sanjun Cai**[1,2] | **Xinxiang Li**[1,2] | **Dawei Li**[1,2]

[1] Department of Colorectal Surgery, Fudan University Shanghai Cancer Center, Shanghai, China

[2] Department of Oncology, Shanghai Medical College, Fudan University, Shanghai, China

[3] Department of Gastrointestinal Surgery, The Second Hospital, Cheeloo College of Medicine, Shandong University, Jinan, China

[4] Department of General Surgery, Shanghai General Hospital, School of Medicine, Shanghai Jiaotong University, Shanghai, China

[5] Cancer Institute, Fudan University Shanghai Cancer Center, Shanghai, China

[6] Department of Pathology, Fudan University Shanghai Cancer Center, Shanghai, China

[7] Department of Biobank, Fudan University Shanghai Cancer Center, Shanghai, China

[8] Department of Oncology, Yijishan Hospital of Wannan Medical College, Wuhu, Anhui, China

Correspondence
Dawei Li, Department of Colorectal Surgery, Fudan University Shanghai Cancer Center, 270 Dong'an Road, Shanghai, 200032, China.
Email: li_dawei@fudan.edu.cn
Xinxiang Li, Department of Oncology, Shanghai Medical College, Fudan University, 270 Dong'an Road, Shanghai, 200032, China.
Email: xinxiangli@fudan.edu.cn

Senlin Zhao, Yushuai Mi, and Binbin Zheng contributed equally to this study.

Funding information
National Nature Science Foundation of China, Grant/Award Numbers: 81772583, 81972293, 82003088, 81802420; Shanghai Sailing Program, Grant/Award Number: 19YF1409600; Nature Science Foundation of Shandong Province, Grant/Award Number: ZR2019PH008

Abstract

Liver metastasis of colorectal cancer (CRLM) is the most common cause of CRC-related mortality, and is typically caused by interactions between CRC cells and the tumour microenvironment (TME) in the liver. However, the molecular mechanisms underlying the crosstalk between tumour-derived extracellular vesicle (EV) miRNAs and the TME in CRLM have yet to be fully elucidated. The present study demonstrated that highly metastatic CRC cells released more miR-181a-5p-rich EVs than cells which exhibit a low metastatic potential, in-turn promoting CRLM. Additionally, we verified that FUS mediated packaging of miR-181a-5p into CRC EVs, which in-turn persistently activated hepatic stellate cells (HSCs) by targeting SOCS3 and activating the IL6/STAT3 signalling pathway. Activated HSCs could secrete the chemokine CCL20 and further activate a CCL20/CCR6/ERK1/2/Elk-1/miR-181a-5p positive feedback loop, resulting in reprogramming of the TME and the formation of pre-metastatic niches in CRLM. Clinically, high levels of serum EV containing miR-181a-5p was positively correlated with liver metastasis in CRC patients. Taken together, highly metastatic CRC cells-derived EVs rich in miR-181a-5p could activate HSCs and remodel the TME, thereby facilitating liver metastasis in CRC patients. These results provide novel insight into the mechanism underlying liver metastasis in CRC.

KEYWORDS
CCL20/CCR6/ERK1/2/Elk-1/miR-181a-5p feedback loop, colorectal liver metastasis, extracellular vesicle, hepatic stellate cell, miR-181a-5p, tumour microenvironment

1 | INTRODUCTION

Colorectal cancer (CRC) ranks second in terms of cancer-related mortality globally, and ~50% of CRC deaths are caused by liver metastases (Beckers et al., 2018). Interactions between tumour cells and the tumour microenvironment (TME), play important roles in the liver metastasis of CRC (CRLM). Accordingly, elucidating the mechanisms involved in the interactions between tumour cells and the TME appear to be of paramount importance in improving our understanding of CRLM.

During CRLM, cancer cells can induce the formation of pre-metastatic niches by remodelling the TME (Illemann et al., 2016; Schütte et al., 2017). As reported, an activated hepatic stellate cell (α-HSC) signature was found to be the most common biological process in secondary or primary liver cancer (Affo et al., 2017; D. Y. Zhang et al., 2016). α-HSCs can transdifferentiate from a state of quiescence into highly proliferative and mobile myofibroblasts (Olaso et al., 1997). Furthermore, α-HSCs can affect the growth and invasion of CRC cells by remodelling and depositing extracellular matrix (ECM) (Ahmad et al., 2003). Thus, exploring the interaction between CRC cells and HSCs, and elucidating the underlying mechanisms may lead to advances in the prevention of CRLM.

Extracellular vesicles (EVs) were previously classified into two primary subtypes based on the mechanisms of biogenesis: endosome-origin small EVs and plasma membrane-derived ectosomes (microvesicles/microparticles) (Olaso et al., 1997), with a diameter ranging from 40 to 160 nm and 50 to 1000 nm, respectively (Ahmad et al., 2003). Characterized by their lipid bilayer membrane and carrying a number of biomolecules, EVs are generally considered as messengers involved in intercellular communication in the TME, and have been shown to play significant roles in the progression of several types of cancer (Fang et al., 2018; Qin et al., 2019). We have previously summarized the biogenesis of EVs that participate in CRC and also committed to research on functional biomarkers as well as molecular mechanisms underlying the crosstalk between cancer cells and the TME of CRLM (Wei et al., 2020; Zhao et al., 2020, 2021). HSCs are the most abundant non-hepatocyte resident cells in the liver and their presence is correlated with CRLM. However, whether CRC-derived EVs regulate HSCs to induce liver metastasis via secretion of miR-rich EVs, and the miRNAs involved in this process remains to be determined.

In this study, we discovered that highly-metastatic CRC cells released miR-181a-5p-rich EVs that contributed to liver metastasis via regulation of the interactions between CRC cells and HSCs, and remodelling of the TME. These findings identified a novel specific biomarker for CRLM and a novel strategy for predicting the risk of secondary liver cancer caused by CRC.

2 | MATERIALS AND METHODS

2.1 | Patients and tissue specimens

A total of 308 patients with CRC between January 2008 and September 2009 and a further 49 patients with CRLM between February 2012 and May 2018, who were diagnosed at Fudan University Shanghai Cancer Center were enrolled in this study; their clinicopathological characteristics are summarized in Supplementary Tables S1 and S2, respectively. Human serum specimens were collected prior to tumour resection, while normal mucosa and paired cancer tissues, as well as metastatic tissues, were collected immediately after surgical resection. Tissue microarray (TMA) including tumour and paired normal tissues from the 308 patients was performed as reported previously (Zhao et al., 2017). Written informed consent was obtained from each patient and the study protocol conformed to the ethical guidelines of the 1975 Declaration of Helsinki and was approved by the Ethics Committee of our institution.

2.2 | EV isolation and analysis

To remove any cell contamination, the supernatant collected from 3-day cell cultures or plasma samples was first centrifuged at 500*g* for 10 min. Subsequently, the supernatant was centrifuged at 12,000*g* for 20 min to remove any possible apoptotic bodies and large cell debris. Subsequently, the EVs were enriched by centrifugation at 100,000*g* for 70 min. Finally, they were rinsed in 20 ml PBS and collected by ultracentrifugation at 100,000*g* for 70 min. The EVs cup-shaped morphology and number were evaluated using a Philips CM120 BioTwin transmission electron microscope (FEI Company, USA) and NanoSight NS300 (Malvern Instruments Ltd., UK), respectively.

Other materials and methods used in this study are described in the Supplementary materials.

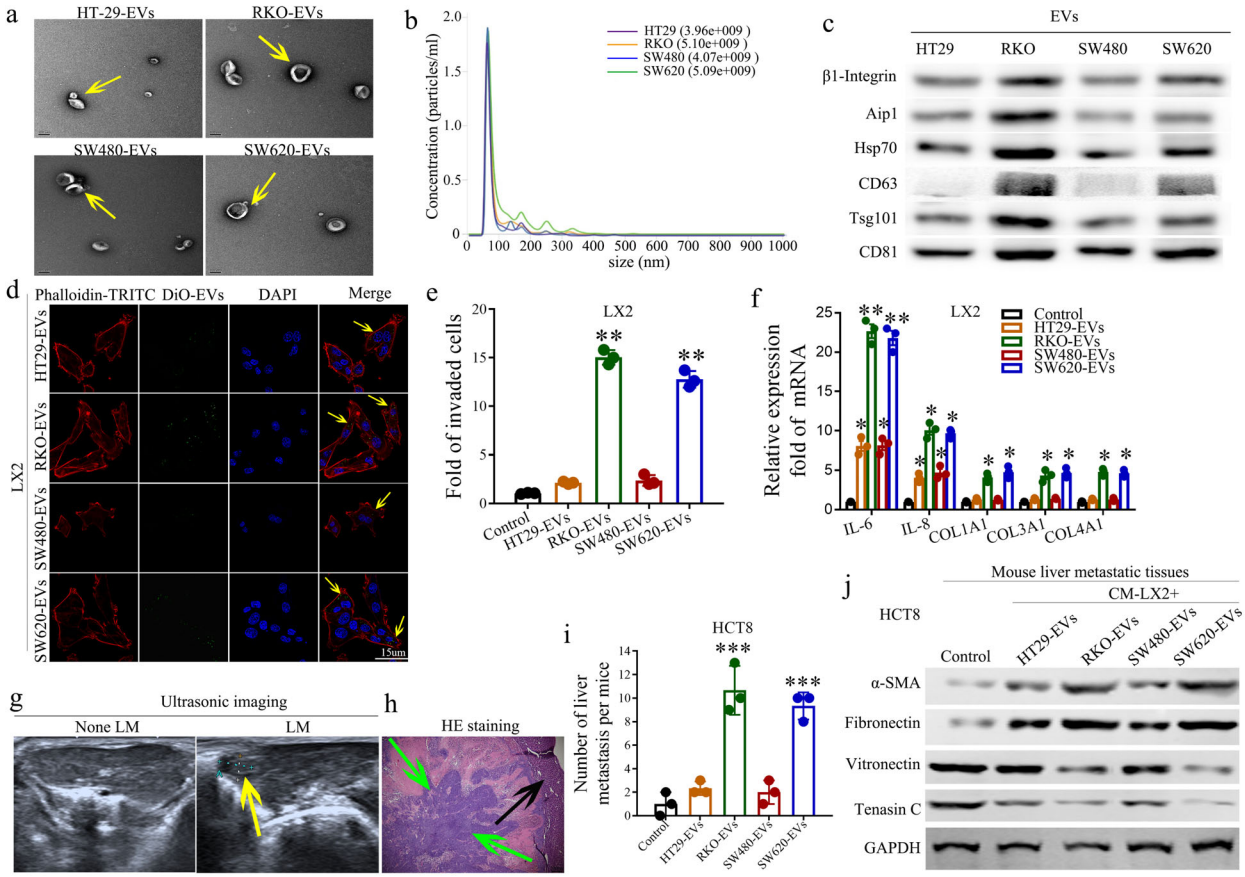

FIGURE 1 **EVs derived from highly metastatic CRC cells mediate the activation of HSCs**. The phenotype of EVs derived from two weakly-metastatic CRC cell lines (HT29 and SW480) and two highly-metastatic CRC cell lines (RKO and SW620) were analyzed by electron microscopy (a) and nanoparticle tracking analysis by Nano Sight (b); yellow arrows indicate representative EVs. (c) WB analysis of typical biomarkers of EVs in the four CRC cell lines. (d) LX2 cells were incubated with DiO-labelled EVs (25 μg/ml) from CRC cell lines (HT29, SW480, RKO, SW620) for 24 h, and representative immunofluorescence images show the delivery of DiO-labelled CRC cell-derived EVs (green) into Dil-labelled LX2 cells (red); yellow arrows indicate EVs. (e) Transwell assays were used to determine the role of EVs (equal quantities) derived from different CRC cells on the invasive ability of LX2 cells; scale bar: 50 μm. (f) The expression levels of pro-inflammatory genes were determined by qPCR in LX2 cells, which were co-cultured with EVs from different CRC cells. (g) Representative images of ultrasound detection of liver metastases 9 weeks after injecting HCT8 cells co-cultured with EVs derived from different CRC cells into the spleens of nude mice. Left panel, without liver metastasis (None LM); right panel, with liver metastasis (yellow arrow, LM). (h) Representative image of HE staining for liver metastases in nude mice (green arrows: metastatic tumour node; black arrow: normal liver cell). (i) Number of metastatic colonies in the livers of nude mice from different groups based on ultrasound detection and HE staining. (j) WB analysis of the ECM proteins (α-SMA, fibronectin, vitronectin and tenascin C) in the liver metastases of mice from each group ($^{*}p < 0.05$; $^{**}p < 0.01$; $^{***}p < 0.001$)

3 | RESULTS

3.1 | EVs derived from highly metastatic CRC cells activate HSCs during CRLM

During liver metastasis, HSCs are usually activated, as determined by the presence of α-SMA-positive myofibroblasts generating ECM. We also observed that metastases to the liver exhibited strong staining for α-SMA (Supplementary Figure S1). We further examined whether CRC cells could activate HSCs via the activity of EVs. Two CRC cell lines with a weak-metastatic potential (HT29 and SW480) and two with highly-metastatic cell lines (RKO and SW620) were selected in the following study, and EVs derived from these four CRC cells were isolated and purified from conditioned medium (CM). Electron microscopy and nanoparticle tracking analysis demonstrated that more EVs were secreted from highly-metastatic CRC cells (Figure 1a and b; Supplementary Figure S2a-d; Table S5). As Hsp70, Tsg101, Aip1, β1-Integrin, Cd81, and Cd63 serve as typical biomarkers for EVs (Conde-Vancells et al., 2008), we detected the proteins extracted from EVs using WB and found that all typical EV markers were present (Figure 1c). Additionally, we also examined the expression of proteins shown to be absent in EVs, such as Calnexin, GM130, Cyto C as well as in cytoplasm, and found that they were not expressed in the CRC cell-derived EVs, which further confirmed that the isolated particles were indeed EVs (Supplementary Figure S2e). Interestingly, highly-metastatic CRC cells secrete a greater quantity of EVs (Figure 1c). To further demonstrate whether CRC cell-derived EVs activated HSCs, LX2 cells were used

as a normal HSC line. HT29/SW480/RKO/SW620 cell-derived EVs were labelled with DiO (green) and LX2 cells were labelled with Dil (red). Immunofluorescence imaging demonstrated the presence of DiO (green) spots in recipient HSCs (Figure 1d, Supplementary Figure S2f), suggesting that labelled EVs released by CRC cells were delivered to HSCs. Notably, highly-metastatic CRC cells could deliver a greater quantity of EVs to HSCs, indicating that highly-metastatic CRC-derived EVs may play key roles in the interactions between HSCs and CRC cells.

In order to investigate the effects of CRC-derived EVs on HSCs, we performed Transwell assays and found that EVs derived from highly-metastatic CRC cells could enhance the invasive ability of LX2 cells in vitro (Figure 1e, Supplementary Figure S2g). During the formation of pre-metastatic niches in metastatic liver cancer, chronic liver inflammation is common (Affo et al., 2017). So we further detected the expression levels of pro-inflammatory genes in LX2 cells following CRC-derived EV stimulation. Interestingly, as shown in Figure 1f, LX2 cells co-cultured with EVs from highly-metastatic CRC cells expressed significantly higher mRNA levels of IL-6, IL-8, COL1A1, COL3A1, and COL4A1 (particularly IL-6) than those co-cultured with EVs from cells with a low metastatic potential. In addition, we found that a larger number of liver metastases were detected following injection of EVs from highly-metastatic CRC cells than from the weakly-metastatic CRC cells by HCT8 cells (Figure 1 g-i, Supplementary Figure S2h), which indicated the potential role of highly-metastatic CRC cell-derived EVs in promoting liver metastasis. Additionally, the expression levels of pro-inflammatory genes were also determined by ELISA in tissues samples from in vivo metastasis experiments, and the results indicated that only IL-6 showed higher expression in LX2 cells co-cultured with EVs from highly-metastatic CRC cells than those from weakly-metastatic CRC cells (Supplementary Figure S2i). The WB analysis showed that EVs from highly-metastatic CRC cells could significantly remodel the liver ECM (α-SMA and fibronectin expression upregulated; vitronectin and tenascin C expression downregulated) (Figure 1j). Together, these data indicated that EVs from highly-metastatic CRC cells could activate HSCs and remodel the liver ECM during CRLM.

3.2 | EVs derived from highly metastatic CRC cells rich in miR-181a-5p activate HSCs

To elucidate whether CRC cell-derived EV miRNAs participated in HSC activation, we first compared the miRNA expression profiles between EVs from different CRC cells using microarrays (Figure 2a; Supplementary Table S6) and uploaded the data to GEO (accession no. GSE141997). Then, we evaluated the expression of 16 miRNAs with ≥5-fold change and $p < 0.001$ using TCGA data. Among them, we chose nine dysregulated miRNAs with a LogFC > 1, $p < 0.001$ and a FDR < 0.05 for further evaluating the prognostic roles of these miRNAs on OS and DFS. As shown in Supplementary Figures S3 and 4, only high expression of miR-181a-5p predicted a poor OS and DFS in 565 CRC patients. Furthermore, we investigated miR-181a-5p expression in the EVs, and found the levels of miR-181a-5p in EVs from highly-metastatic CRC cells were significantly higher than those from weakly-metastatic CRC cells (Figure 2b). Accordingly, we chose miR-181a-5p as the candidate miRNA for further analysis in the present study. As shown in Figure 2c, the expression levels of miR-181a-5p in LX2 cells incubated with CM from highly-metastatic CRC cells were notably higher than those with EV-depleted CM using GW4869, an inhibitor of EV secretion. Furthermore, following transient transfection with Cy3 (red)-tagged miR-181a-5p, CRC cell-derived EVs were co-cultured with LX2 cells and fluorescently labelled miR-181a-5p was detected in LX2 cells (Figure 2d), suggesting that miR-181a-5p was transferred from CRC cells to HSCs via EVs, with a greater quantity of miR-181a-5p transferred from highly-metastatic CRC cells. Notably, the levels of miR-181a-5p in the CM of CRC cells remained unchanged upon RNase A treatment, whilst significantly decreasing following treatment with RNase A plus Triton X-100 (Supplementary Figure S5a), which indicated that extracellular miR-181a-5p was primarily encased within a membrane rather than directly released. Also of interest, miR-181a-5p levels were almost equal between EVs and whole CRC-cell CM (Supplementary Figure S5b). Accordingly, these results strongly supported the hypothesis that miR-181a-5p may activate HSCs via CRC cell-derived EVs.

Subsequently, Transwell assays revealed that the number of invading LX2 cells in the transfected miR-181a-5p mimics group was greater than that of the control group (Figure 2e, Supplementary Figure S5c). Moreover, transfecting miR-181a-5p mimic resulted in increased mRNA levels of IL-6 and IL-8 (particularly IL-6) in LX2 cells (Figure 2f). Highly-metastatic CRC cells were transfected with anti-miR-181a-5p, then EVs were obtained and added to LX2 cells. Transwell assays demonstrated that anti-miR-181a-5p may attenuate the enhancing effect of highly metastatic CRC cell-derived EVs on the activation of LX2 cells (Figure 2g and h). Together, these results suggest that CRC cell-derived EV miR-181a-5p could promote the activation of HSCs.

3.3 | miR-181a-5p transfer into EVs is regulated by FUS

It has been widely reported that EV-mediated secretion of RNAs requires a specific and selective RNA-binding protein for transport (Cook et al., 2011). By analyzing the database of RNA-binding protein specificities (RBPDB, http://rbpdb.ccbr.utoronto.ca/) (Cook et al., 2011), we retrieved the specific interaction between miR-181a-5p sequence and the motifs of RBPDB to predict potential RBPs regulating miR-181a-5p packaging into EVs. As shown in Supplementary Figure S6a, the motifs of the FUS RNA-binding protein (FUS) and muscle blind-like splicing regulator 1 (MBNL1) displayed specific miR-181a-5p binding sites, with

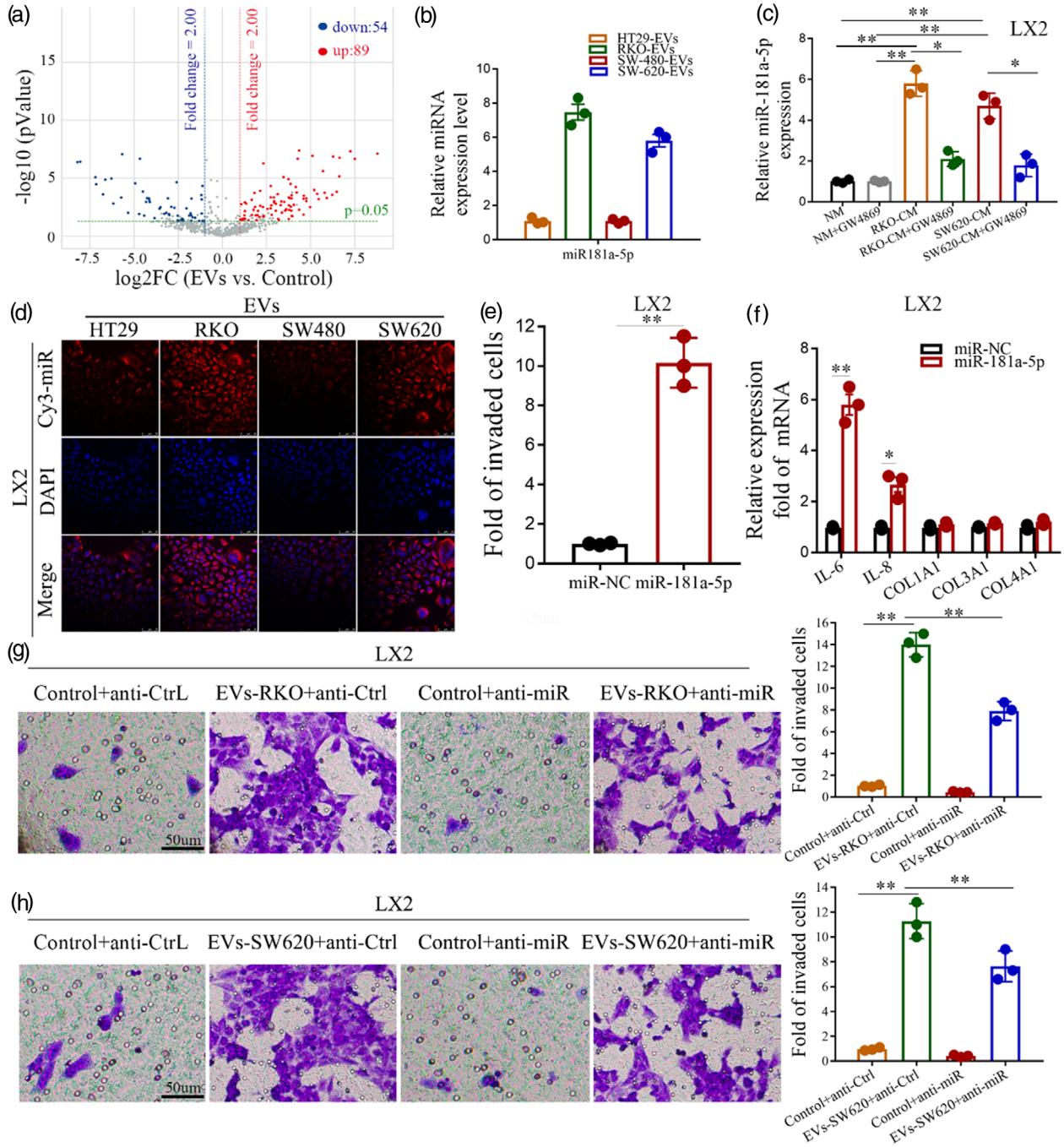

FIGURE 2 **Highly metastatic EVs rich in miR-181a-5p derived from CRC cells regulate the activation of HSCs**. (a) Microarray analysis of the miRNA expression profiles between EVs from highly-metastatic CRC cells and those from weakly-metastatic CRC cells; the data have been uploaded to GEO (accession no. GSE141997). (b) The expression levels of miR-181a-5p in EVs derived from different CRC cell lines were detected by qPCR. (c) LX2 cells were incubated with normal medium (NM), normal medium with EVs-depleted using an inhibitor of EV secretion (GW4869), or conditioned medium (CM) from RKO/SW620 cells with or without EVs-depleted. Then miR-181a-5p expression levels were examined by qPCR. (d) LX2 cells were co-cultured with EVs derived from HT29/SW480/RKO/SW620 pre-transfected with Cy3-tagged miR-181a-5p (red), and the red fluorescence signals in LX2 cells were detected by confocal microscopy. (e) Transwell assays were used to evaluate the effects of exogenous miR-181a-5p on the invasive ability of LX2. (f) qPCR analysis of the effects of exogenous miR-181a-5p on the expression of pro-inflammatory genes in LX2. (g and h) Transwell assays were used to determine the role of EVs derived from highly-metastatic CRC cells (RKO and SW620) and anti-miR-181a-5p constructs in the regulation of the invasive ability of LX2 cells in vitro ($^{*}p < 0.05$; $^{**}p < 0.01$)

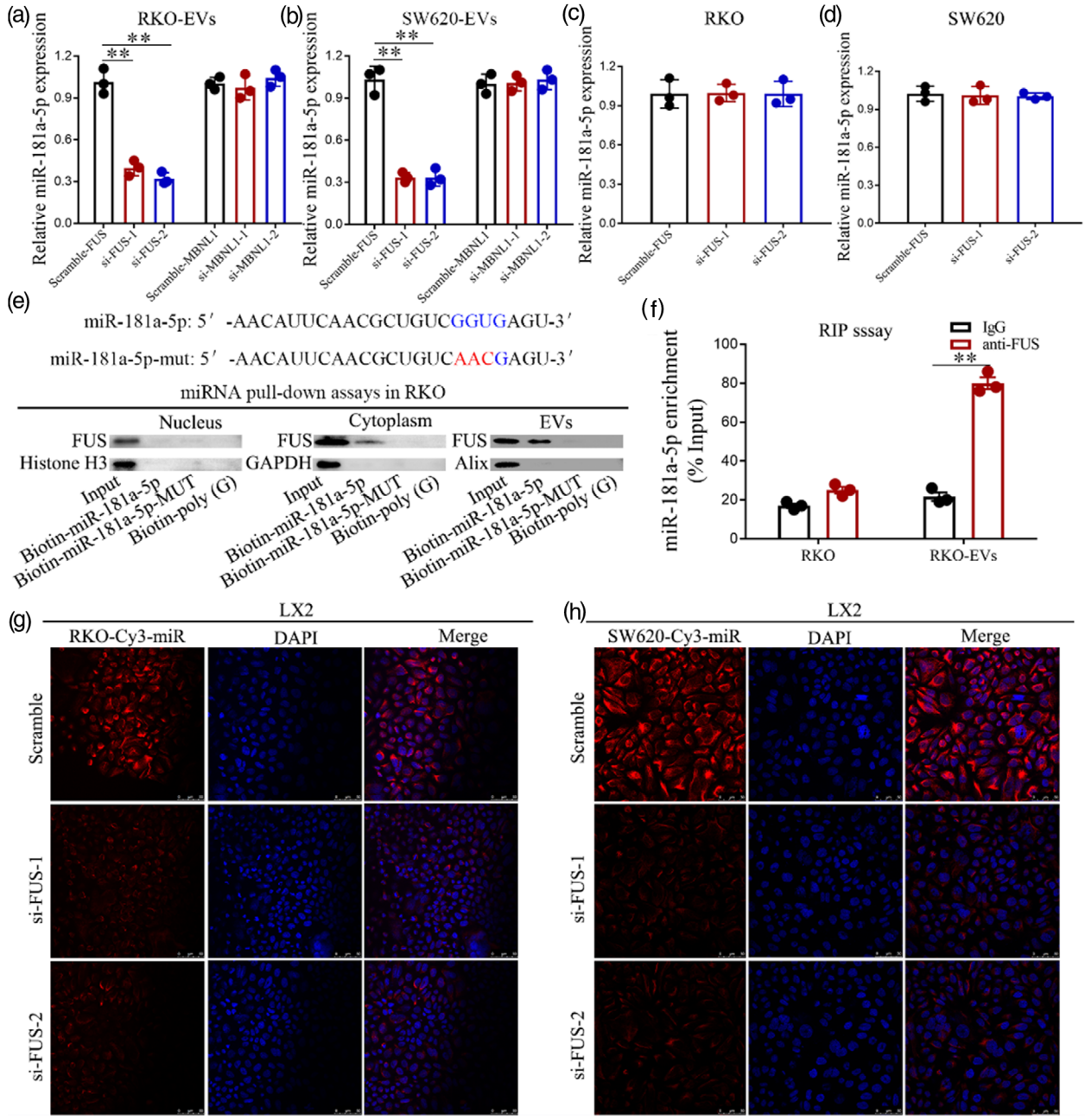

FIGURE 3 **FUS regulates miR-181a-5p transfer into EVs derived from highly metastatic CRC cells**. qPCR analysis of the expression levels of miR-181a-5p in RKO/SW620-derived EVs (a and b) and RKO/SW620 cells (c and d) upon FUS/MBNL1 knockdown. (e) WB analysis of the association between biotinylated wild-type or mutated miR-181a-5p and FUS expression in samples derived by miRNA pull-down performed with nuclear, cytoplasmic or EV lysates from RKO cells; biotinylated poly(G) was used as the negative control. (f) RIP assays with anti-FUS antibody were performed on RKO-conditioned media (CM) and RKO-derived EVs, with IgG serving as the negative control. Then, qPCR was used to analyze the expression levels of miR-181a-5p in immunoprecipitated samples as percentages with respect to the input sample (% input). (g and h) The red fluorescence signals in LX2 cells co-cultured with CM from RKO/SW620 cells transfected with Cy3-miR-181a-5p (red) and si-FUS were detected by confocal microscopy ($^{*}p < 0.05$; $^{**}p < 0.01$)

relative scores >90%. However, we observed that only cells with FUS expression knocked-down exhibited decreased expression levels of EV miR-181a-5p (Figure 3a-d; Supplementary Figure S6b-e), while the expression levels of FUS in the upper four CRC cells did not exhibit a significant decrease (Supplementary Figure S6f, g). Furthermore, miRNA pull-down assays revealed that miR-181a-5p and FUS did bind in the cytoplasm and EVs, but not in the nucleus, and this binding could be abrogated by mutating the binding sequence (GGUG) in miR-181a-5p (Figure 3e; Supplementary Figure S6h). Subsequently, RNA immunoprecipitation assays demonstrated that miR-181a-5p exhibited notably higher enrichment in the FUS antibody group than the IgG group, both in CRC cells and their EV lysates (Figure 3f; Supplementary Figure S6i). Additionally, cell immunofluorescence assays showed that the process of miR-181a-5p transfer from highly-metastatic CRC cells to HSCs via EVs was inhibited by knockdown of

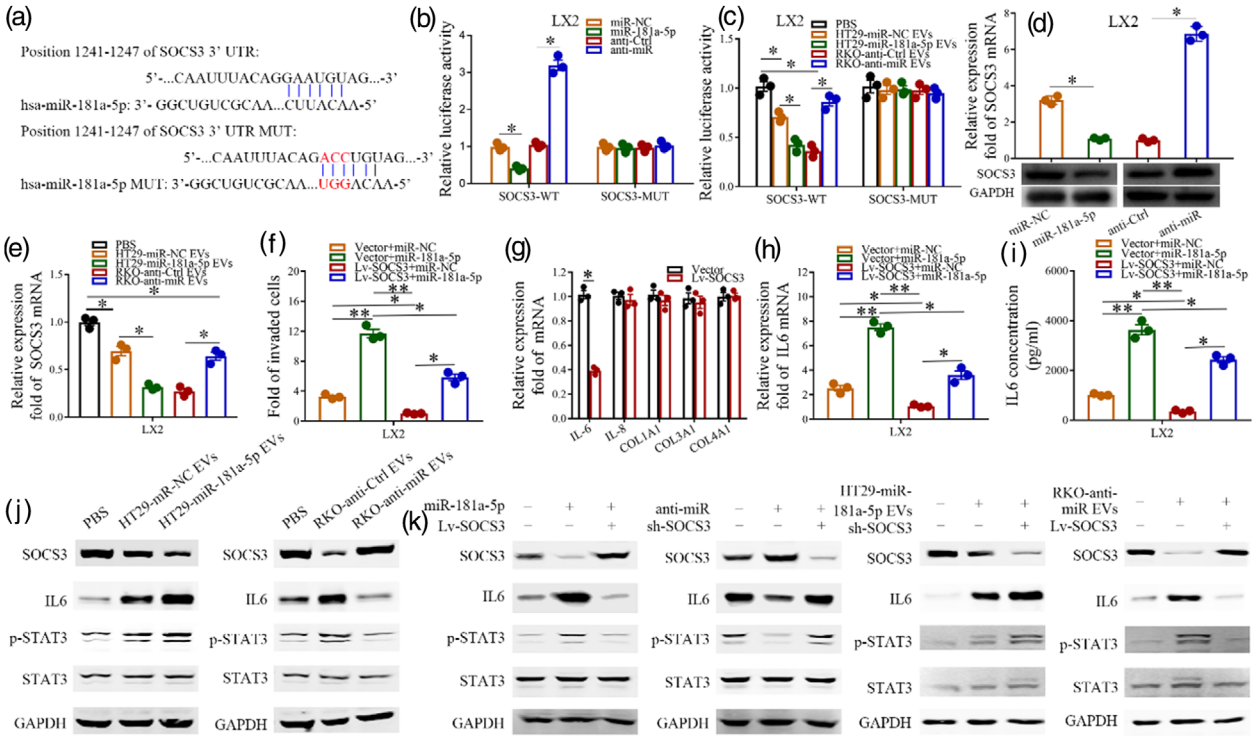

FIGURE 4 **miR-181a-5p rich EVs derived from highly metastatic CRC cells activate HSCs by targeting SOCS3 via the IL6/STAT3 signalling pathway**. (a) Predicted binding sites between miR-181a-5p and the 3′-UTR of the wild-type and mutant SOCS3 gene. (b) The effect of miR-181a-5p mimic and anti-miR-181a-5p constructs on the luciferase activity of the 3′-UTR binding of the wild-type or mutant SOCS3, respectively, in LX2 cells was assessed using a luciferase reporter gene activity assay. (c) LX2 cells were co-cultured with EVs derived from HT29 or RKO cells, which were pre-transfected with miR-181a-5p mimic or anti-miR-181a-5p constructs, respectively. Luciferase reporter gene activity assays were used to detect the effect of EVs derived from CRC cells on the luciferase activity of miR-181a-5p binding with the 3′-UTR of the wild-type or mutant SOCS3 construct in LX2 cells. (d) qPCR and WB analysis were used to examine the effects of exogenous miR-181a-5p on SOCS3 expression in LX2 cells. (e and f) qPCR analysis was used to examine the effect of EVs derived from HT29 and RKO CRC cells rich in miR-181a-5p on SOCS3 expression in LX2 cells. LX2 cells were successively transfected with miR-181a-5p mimic, Lv-SOCS3 or their respective controls. (g) Transwell assays were applied to verify the combined effect of miR-181a-5p and SOCS3 overexpression on the invasion of LX2. (h and i) The combined effects of miR-181a-5p and SOCS3 overexpression on IL6 expression in the cell media was determined using qPCR (h) and ELISA (i), respectively. (j) WB analysis was used to examine the effect of EVs derived from CRC cells rich in miR-181a-5p on the IL6/STAT3 pathway components in LX2. (k) LX2 cells were pre-transfected with miR-181a-5p mimic, anti-miR-181a-5p constructs or HT29/RKO-derived EVs, and then co-cultured with Lv-SOCS3 or sh-SOCS3, respectively. The combined effects of exogenous miR-181a-5p/LvSOCS3, anti-miR-181a-5p/sh-SOCS3, HT29-derived EVs/sh-SOCS3 and RKO-derived EVs/Lv-SOCS3 on the expression of IL6/STAT3 pathway components were determined by WB analysis, respectively ($^{*}p < 0.05$; $^{**}p < 0.01$)

FUS expression in RKO and SW620 cells (Figure 3g and h). Therefore, we demonstrated that FUS could mediate miR-181a-5p packaging into EVs in CRC cells and then transfer EVs containing miR-181a-5p to HSCs by binding to its GGUG sequence.

3.4 | CRC cell-derived EV miR-181a-5p activates HSCs directly by targeting SOCS3 and activating the IL6/STAT3 signalling pathway in HSCs

To further explore the mechanisms by which CRC cell-derived EVs miR-181a-5p was involved in activating HSCs during CRLM, GO/KEGG enrichment analysis was performed and the results showed that miR-181a-5p participated in the development of CRC and also in the regulation of transcription factor complex (Supplementary Figure S7a, b; Tables S7, S8). Furthermore, data from TargetScan Human version 7.2 demonstrated that there was an alignment between the miR-181a-5p sequence and the 3′-UTR of suppressor of cytokine signalling 3 (SOCS3) sequence, suggesting that CRC cell-derived EVs miR-181a-5p may target SOCS3 during the activation of HSCs (Figure 4a). In the present study, we demonstrated that IL6 exhibited the most notable differential expression among the different CRC cell line-derived EVs, and IL6 has also been reported to be involved in the regulation of miRNAs in cancer-related inflammation (Rokavec et al., 2014). Additionally, SOCS3 is frequently inactivated and results in the activation of inflammatory IL6/STAT3 signalling pathway (Lesina et al., 2011; Yasukawa et al., 2003). Thus, it was hypothesized that CRC cell-derived EV miR-181a-5p may activate HSCs via SOCS3-mediated activation of the IL6/STAT3 signalling pathway. Following co-transfection with miR-181a-5p mimic, anti-miR-181a-5p constructs and their respective controls, luciferase vectors with wild-type or mutant versions of the binding sites were used for further verification. As shown in Figure 4b, compared

with the control groups, luciferase activity in LX2 cells transfected with miR-181a-5p mimic or anti-miR-181a-5p constructs was markedly reduced or elevated in the group co-transfected with SOCS3 wild-type binding site vector compared with the SOCS3 mutant-type binding site vector, respectively. Furthermore, similar expression trends were found when LX2 cells were co-cultured with EVs derived from HT29/RKO cells pre-transfected with miR-181a-5p mimics or anti-miR-181a-5p constructs, respectively (Figure 4c). Then in LX2 cells, both at the mRNA and the protein levels, we also demonstrated that overexpression or knockdown of miR-181a-5p significantly inhibited or promoted SOCS3 expression compared with their negative controls (Figure 4d), respectively, with similar expression patterns found when LX2 cells were pretreated with EVs derived from HT29/RKO cells pre-transfected with miR-181a-5p mimic or anti-miR-181a-5p (Figure 4e). Transwell assays demonstrated that overexpression of SOCS3 reduced the number of invading LX2 cells, partly weakening the enhancing effect of miR-181a-5p on the invasion of LX2 cells (Figure 4f; Supplementary Figure S8a). However, only the expression of the pro-inflammatory gene IL-6 was decreased upon SOCS3 overexpression in LX2 cells (Figure 4g). More importantly, SOCS3 overexpression in LX2 cells could counteract the promotive effect of miR-181a-5p on the levels of IL6 in cells and their supernatant (Figure 4h and i). Taken together, these results indicate that exogenous miR-181a-5p can downregulate SOCS3 expression by targeting its 3′-UTR in LX2 cells.

Furthermore, HT29/RKO cells were first pre-transfected with miR-181a-5p mimic or anti-miR-181a-5p, respectively, then LX2 cells were co-cultured with EVs derived from the aforementioned cells. WB assays revealed that CRC cells-derived EV miR-181a-5p markedly promoted the expression of IL6 and p-STAT3, while inhibiting SOCS3 expression in LX2 cells (Figure 4j). However, SOCS3 overexpression or knockdown in LX2 cells could partially neutralize the promotive or inhibitory effect of CRC cell-derived EV miR-181a-5p or anti-miR-181a-5p on the expression of IL6 and p-STAT3 (Figure 4k). Notably, we also showed that CRC cell-derived EV miR-181a-5p significantly increased the expression of α-SMA in LX2 cells (Supplementary Figure S8b). These data indicated that EV miR-181a-5p activated HSCs directly by targeting SOCS3 via activation of the IL6/STAT3 signalling pathway.

3.5 | HSCs activated by CRC-derived EV miR-181a-5p facilitate CRLM in return

As reported, α-HSCs are responsible for remodelling and depositing tumour-associated ECM, and have been shown to be involved in the migration and growth of CRC cells (Eveno et al., 2015). Accordingly, we investigated whether α-HSCs could also promote CRLM in return. We used two different CRC cell lines, HCT-8 and LoVo, for these experiments. LX2 cells were first transfected with miR-181a-5p mimic or the respective control, then CM was added to the upper two CRC cell lines. in vitro Transwell assays revealed that exogenous miR-181a-5p could notably promote the migration and invasion of CRC cells (Figure 5a and b). Next, LX2 cells were first co-cultured with EVs derived from HT29/RKO cells, which had been pre-transfected with miR-181a-5p mimics or anti-miR-181a-5p constructs, then the collected CM was added to the HCT8 and LoVo cells, respectively. in vitro Transwell assays (Figure 5c and d; Supplementary Figure S9a and b) and the in vivo liver metastatic mouse model (Figure 5e-g; Supplementary Figure S9c) all showed that α-HSCs, which were activated by CRC cell-derived EV miR-181a-5p, also facilitated CRC cell migration, invasion and the formation of metastatic tumour colonies in the liver in turn, consistent with our hypothesis. We further examined the expression of ECM components in the metastases to the liver from mice using WB analysis and IHC staining. The results showed that CRC cell-derived EV miR-181a-5p remodelled the liver ECM, by increasing the expression of α-SMA and fibronectin, while reducing the expression of vitronectin and tenascin C (Figure 5h and Supplementary Figure S9d). Additionally, we also performed IHC staining to examine the expression of ECM components in the metastases to the liver of CRLM patients with high/low expression levels of miR-181a-5p. We found that CRLM patients with higher expression levels of miR-181a-5p also displayed stronger staining of α-SMA and fibronectin, but weaker or negative staining of vitronectin and tenascin C (Supplementary Figure S9e). Accordingly, we showed that CRC cell-derived EV miR-181a-5p could remodel the pre-metastatic niche during CRLM.

3.6 | Activated HSCs promote CRLM via activation of the CCL20/CCR6 axis in CRC

As chemokines have been found to be significantly upregulated in several types of cancer, promoting cancer progression within the TME, and as α-HSCs may secrete pro-inflammatory signals including chemokines (Brenner et al., 2013; Kadomoto et al., 2020), we speculated that α-HSCs may promote CRLM via secretion of chemokines. Therefore, using a human chemokine screening test kit, we first tested the levels of chemokines in LX2 cells, which were pre-cultured with RKO cell-derived EVs or a negative control. The results showed that among all the detected chemokines, CCL20, CCL24, and CXCL10 were the top most significantly differentially expressed chemokines (Figure 6a). Furthermore, when miR-181a-5p was overexpressed in LX2 cells, we found that the expression difference of CCL20 was considerably more significant than that of CCL24 and CXCL10 (Figure 6b; Supplementary Figure S10a and b). Next, we cultured LX2 cells with EVs derived from HT29/RKO cells, which were pre-transfected with miR-181a-5p mimic or anti-miR-181a-5p constructs, respectively, and tested the expression levels of CCL20 by ELISA. As shown in Figure 6c, overexpression or knockdown of miR-181a-5p could partially enhance or neutralize

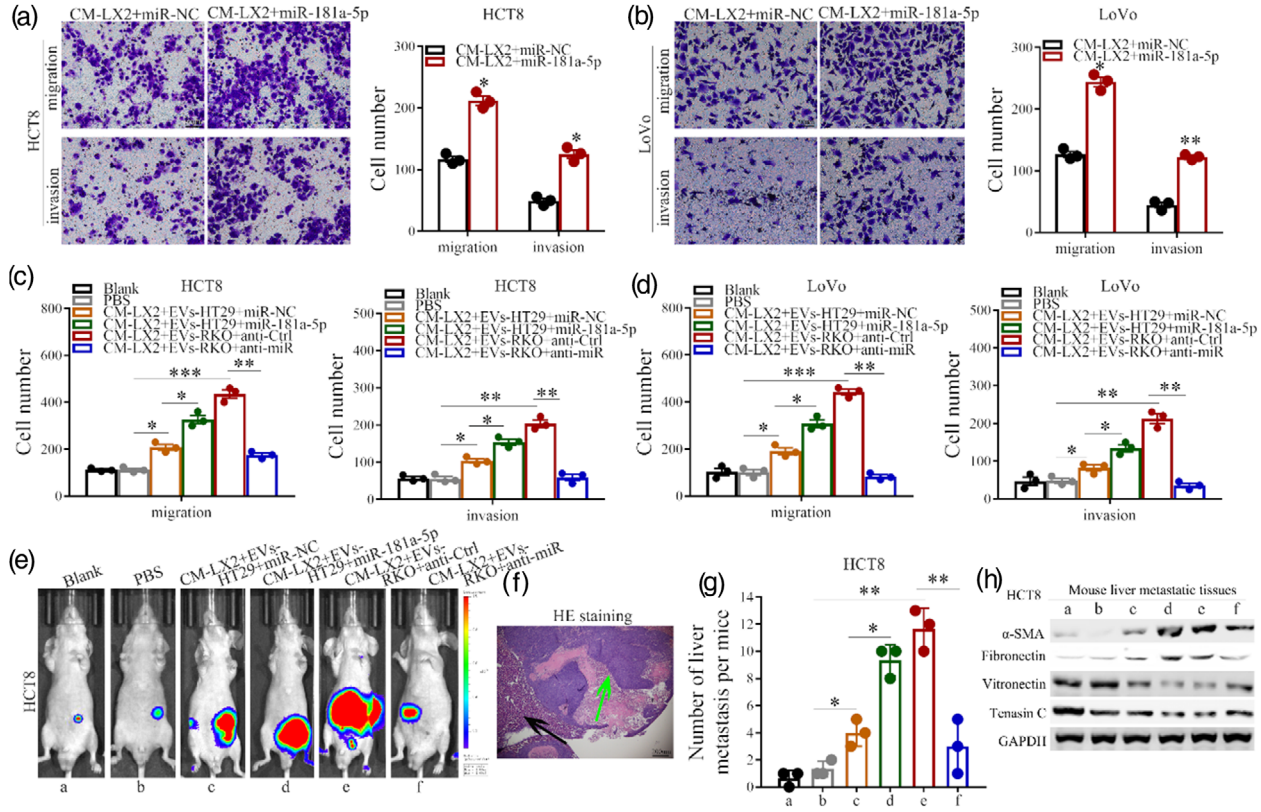

FIGURE 5 **HSCs activated by EVs** rich in **miR-181a-5p derived from CRC cells** promote CRC cell migration and invasion in vitro and liver metastasis in vivo. (a and b) LX2 cells were first transfected with miR-181a-5p mimic or the respective control. Then, CM from these transfected LX2 cells were added to HCT8/LoVo cell cultures, and transwell assays were used to examine the effect of exogenous miR-181a-5p on the migration and invasion of CRC cells. (c and d) HT29/RKO cells were pre-transfected with miR-181a-5p mimic or anti-miR-181a-5p constructs, respectively. EVs were isolated and LX2 cells were co-cultured with these EVs. Then the CM of these LX2 cells was added to HCT8/LoVo cells, respectively. The effect of α-HSCs on the migration and invasion of CRC cells was determined using transwell assays in vitro (c and d) and liver metastasis of nude mice by live imaging in vivo (e). Representative images of live imaging (e) and HE staining (f) of the liver metastases in nude mice (green arrows: metastatic tumour node; black arrow: normal liver cell). (g) Number of metastatic colonies in the livers of the nude mice from different groups based on live imaging and HE staining. (h) WB analysis of the protein expression levels of ECM proteins (α-SMA, fibronectin, vitronectin and tenascin C) in the metastases to the liver in the mice ($^{*}p < 0.05$; $^{**}p < 0.01$)

the promotive effects of HT29/RKO cell-derived EVs on the secretion of CCL20 in LX2 cells, respectively. As CCL20 is a chemoattractant that promotes chemotaxis of cells expressing CCR6, we further evaluated CCR6 expression in CRC by IHC staining and found that CCR6 staining in CRC tissues was notably stronger than in the normal tissues, indicating that CCL20 secreted by LX2 cells may exert a function on CRC cells (Figure 6d).

To further investigate the role of the CCL20/CCR6 axis in CRLM, LX2 cells were first transfected with miR-181a-5p mimic and treated with anti-CCL20 antibody or IgG, and then co-cultured with HCT8/LoVo cells. Additionally, after transfection with miR-181a-5p mimic, LX2 cells were also co-cultured with HCT8/LoVo cells with CCR6 expression knocked down rather than treatment with an anti-CCL20 antibody or IgG. It was demonstrated that the inhibition of the CCL20/CCR6 axis could partially counteract the enhancing role of α-HSCs, which were activated by CRC cell-derived EV miR-181a-5p, on CRC cell migration, invasion and liver metastasis in vitro and in vivo (Figure 6e-i; Supplementary Figure S11). Together, the above results showed that CRC cell-derived EV miR-181a-5p could activate HSCs, and α-HSCs in turn promoted CRLM via activation of a CCL20/CCR6 axis in CRC.

3.7 | A CCL20/CCR6/ERK1/2/Elk-1/miR-181a-5p positive feedback loop mediates the interaction between HSCs and CRC cells during CRLM

When the CM of LX2 cells pre-transfected with miR-181a-5p mimic was added to HCT8 and LoVo cells, we found that α-HSCs could upregulate the expression of miR-181a-5p in CRC cells (Figure 7a). Interestingly, the above phenomena was abrogated by treatment with an anti-CCL20 antibody in CRC cells (Figure 7a). These findings indicated that α-HSCs could affect the functions of CRC cells via CCL20. As reported previously, the CCL20/CCR6 axis can promote cancer progression through the

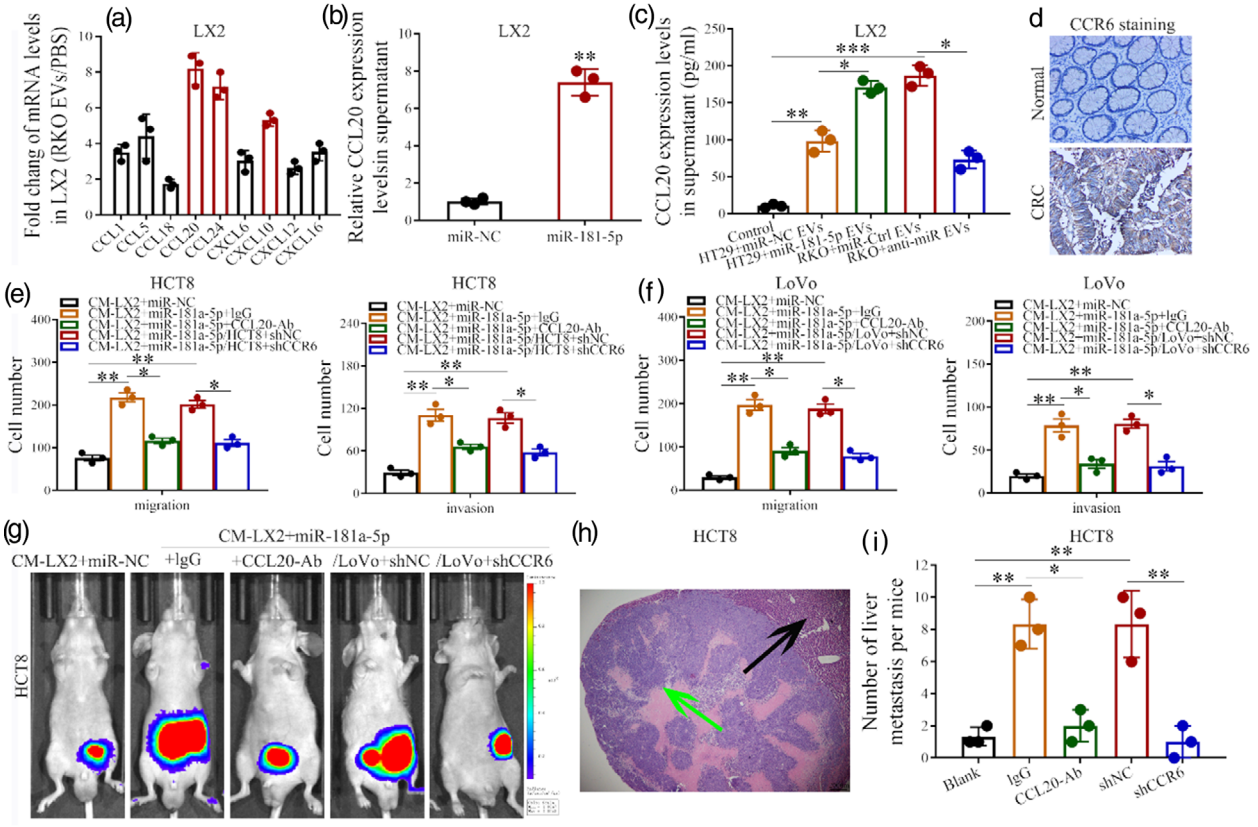

FIGURE 6 **Activated HSCs promote CRC liver metastasis via the CCL20/CCR6 axis**. (a) The levels of chemokines in LX2 cells pre-cultured with EVs derived from RKO cells or a negative control, were tested using a human chemokine screening test kit. (b and c) The effect of exogenous miR-181a-5p (b) and highly metastatic CRC cell-derived EV miR-181a-5p (c) on the expression of CCL20 in LX2 cells was assessed using ELISA. (d) IHC staining of CCR6 in CRC; scale bar: 200 μm. (e-i) LX2 cells were first transfected with miR-181a-5p mimic or treated with an anti-CCL20 antibody with IgG as a negative control, then co-cultured with HCT8/LoVo cells. After transfection with miR-181a-5p mimic, LX2 cells were also co-cultured with HCT8/LoVo cells that had had CCR6 expression knocked down rather than being treated with an anti-CCL20 antibody or IgG control. Next, the effects of the CCL20/CCR6 axis on the migration and invasion of CRC cells were determined using in vitro Transwell assays (e and f), as well as on metastasis to the liver in vivo using live imaging (g). Representative images of live imaging (g) and HE staining (h) of liver metastases in nude mice (green arrows: metastatic tumour node; black arrow: normal liver cell). (i) Number of metastatic colonies in the livers of nude mice from different groups based on live imaging and HE staining ($^{*}p < 0.05$; $^{**}p < 0.01$)

MAPK signalling pathway (Kadomoto et al., 2020; Li et al., 2007). To confirm the mechanism by which miR-181a-5p upregulation increased CCL20 release from α-HSCs, we first performed WB in HCT8 and LoVo cells pretreated with CCL20 or transfected with shCCR6. It was found that the CCL20/CCR6 axis only promoted the phosphorylation of ERK1/2 compared with the control groups, but did not affect JUK or p38 phosphorylation, indicating that CCL20 secreted from α-HSCs may upregulate miR-181a-5p via activation of the ERK1/2 signalling pathway in CRC cells in a CCR6-dependent manner (Supplementary Figure S12a). Subsequently, when an inhibitor of the ERK1/2 signalling pathway (PD98059) was added to the HCT8/LoVo cells co-cultured with the CM of LX2, which were pre-transfected with miR-181a-5p mimic, the expression levels of miR-181a-5p were evidently decreased, suggesting that miR-181a-5p may also be positively regulated by the ERK1/2 signalling pathway through a positive feedback loop (Figure 7b).

As ERK1/2 translocates to the nuclei and promotes transcription of its target genes, we knocked down six candidate transcription factors, and found that silencing of only Elk-1 notably downregulated miR-181a-5p expression and suppressed α-HSCs-induced miR-181a-5p expression in CRC cells (Figure 7c and d; Supplementary Figure S12b and c and Figure S13). LX2 cells were first transfected with miR-181a-5p mimic, or treated with an anti-CCL20 antibody or IgG control, and co-cultured with HCT8/LoVo cells. Additionally, after transfection with miR-181a-5p mimic, LX2 cells were also co-cultured with HCT8/LoVo cells with CCR6 expression knocked down rather than being treated with anti-CCL20 antibody or IgG control antibody. As shown in Figure 7e, α-HSCs could promote the activation of the ERK1/2 signalling pathway, however, inhibition of the CCL20/CCR6 axis inhibited α-HSC-mediated activation of the ERK1/2 signalling pathway. Furthermore, we demonstrated that α-HSCs facilitated the phosphorylation of ERK1/2 and Elk-1, which could be abrogated by treatment with an CCL20 antibody and PD98059 (Figure 7f). Accordingly, we hypothesized that the activation of the ERK1/2 signalling pathway may upregulate miR-181a-5p through the transcriptional function of Elk-1 in CRC. To confirm this hypothesis, we first predicted the potential transcriptional binding regions and specific binding sites using the tool LASAGNA-Search 2.0 as well as the human genomic databases of the National

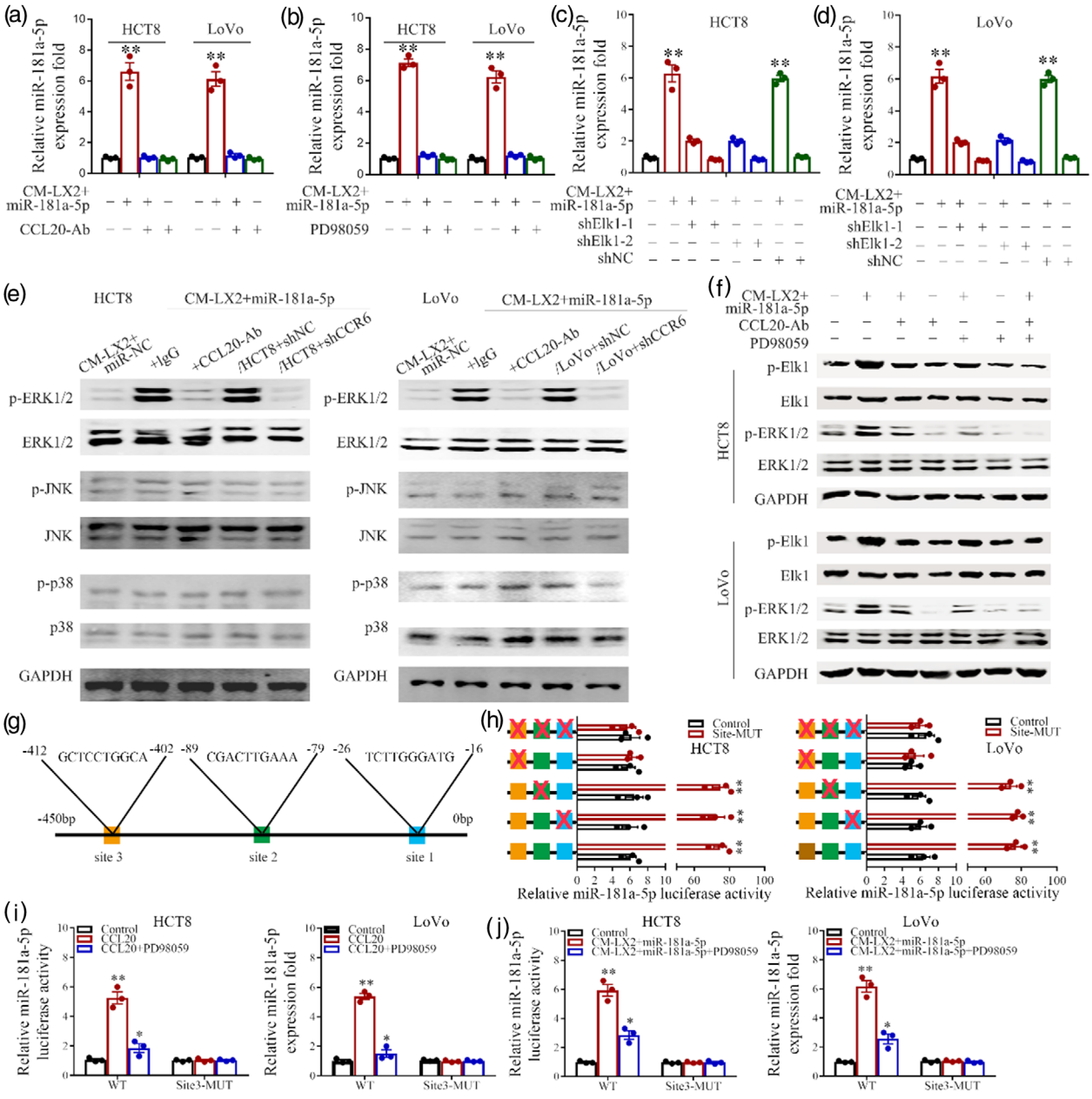

FIGURE 7 **A** CCL20/CCR6/ERK1/2/Elk-1/miR-181a-5p positive feedback loop mediates the interaction between HSCs and CRC cells during CRLM. (a) LX2 cells were pre-transfected with miR-181a-5p mimic, and the CM as well as CCL20 antibody were added to HCT8 and LoVo cells, respectively, to determine the combined effect of activated HSCs and CCL20 on the expression of miR-181a-5p in CRC cells. (b) The inhibitor of the ERK1/2 signalling pathway (PD98059) and CM of LX2 cells that had been pre-transfected with miR-181a-5p mimic, was added to HCT8/LoVo cells, respectively. The transfection efficiency was assessed by qPCR. (c and d) LX2 cells were pre-transfected with miR-181a-5p mimic, and their CM was added to HCT8 (c) and LoVo (d) cells with Elk-1 expression knocked down, respectively, then the expression of miR-181a-5p on CRC cells was examined by qPCR. (e) LX2 cells were first transfected with miR-181a-5p mimic or treated with an anti-CCL20 antibody with IgG as a negative control, and then co-cultured with HCT8/LoVo cells. Additionally, after transfection with miR-181a-5p mimic, LX2 cells were also co-cultured with HCT8/LoVo cells following CCR6 knockdown. WB assays were used to demonstrate the expression levels of MAPK pathway components, respectively. (f) The combined effect of activated HSCs, CCL20 antibody as well as PD98059 on the activation of ERK1/2 and Elk-1 were further verified by WB. (g) Schematic diagram of the three specific binding sites between Elk-1 and the promoter of miR-181a-5p based on LASAGNA-Search 2.0 and human genomic databases from NCBI. (h) The binding site truncation mutants and their control vectors were cloned into pGL3-luciferase reporter plasmids and transfected into HCT8/LoVo cells. A luciferase reporter gene activity assay was used to analyze the changes in luciferase activity and determine the transcriptional sites. (i) A luciferase reporter gene activity assay was further used to analyze the combined effects of exogenous CCL20 and PD98059 on the luciferase activity of the wild-type/mutant Elk-1 on binding site 3 of the miR-181a-5p promoter constructs in HCT8/LoVo cells. (j) qPCR was used to determine the effects of PD98059 on the RNA levels of miR-181a-5p in HCT8/LoVo, which had been co-cultured with CM from LX2 cells overexpressing miR-181a-5p ($^{*}p < 0.05$; $^{**}p < 0.01$)

Center for Biotechnology Information. There were three specific binding sites between Elk-1 and the promoter of miR-181a-5p (Supplementary Figure S14). Subsequently, we constructed wild-type and mutant variants with the binding site mutated, and a luciferase reporter gene assay was used to confirm the transcriptional effect of Elk-1 on the promoter of miR-181a-5p in HCT8 and LoVo, respectively (Figure 7g; Supplementary Table S9). We discovered that only mutant binding site 3 could downregulate luciferase reporter gene activity of miR-181a-5p and inhibit miR-181a-5p transcriptional expression (Figure 7h). Moreover, we demonstrated that the promotive role of CCL20 and α-HSCs on the expression of miR-181a-5p in CRC cells could be inhibited by treatment with an ERK1/2 signalling pathway inhibitor; however, these processes were abolished when binding site 3 was mutated in HCT8/LoVo cells (Figure 7i and j). To further understand the potential crosstalk between CRC cells and HSCs in vivo, we first selected a liver metastatic mouse model and also liver metastatic tissues from CRLM patients. For the mouse liver metastatic model, LX2 cells were first co-cultured with EVs derived from HT29/RKO cells, which had been pre-transfected with miR-181a-5p mimic or anti-miR-181a-5p constructs, respectively, then their CM was added to HCT8 cultures, and these HCT8 cells were injected into the spleens of male BABL/c nude mice to establish the mouse model of CRLM. Tissues of metastases to the liver from CRLM patients were randomly selected from patients with high or low miR-181a-5p expression. Then, manual multicoloured immunofluorescence staining was used to detect the expression levels of α-SMA, p-STAT3 and p-ERK in mice as well as in the CRC patients' metastatic liver tissues. The results showed that p-STAT3 was primarily detected in HSCs with positive expression of α-SMA, while p-ERK was primarily observed in the tumour cells of the metastases to the liver (Supplementary Figure S15). Furthermore, we discovered that miR-181a-5p in EVs derived from CRC cells notably increased the expression of α-SMA and p-STAT3 in HSCs, and this was also positively correlated with strong p-ERK staining in mice metastatic colonies in the liver, compared with the respective control groups (Supplementary Figure S15a). Manual multicoloured immunofluorescence staining in human tissues of metastases to the liver showed that CRLM patients with higher expression levels of miR-181a-5p also presented stronger staining of α-SMA and p-STAT3 in HSCs and p-ERK in the metastases to the liver compared with those with lower miR-181a-5p expression (Supplementary Figure S15b). Accordingly, these data confirm that miR-181a-5p in EVs regulated crosstalk between CRCs and HSCs within the CRLM metastatic microenvironment in vivo. Taken together, activation of the ERK1/2/Elk-1 signalling pathway may also promote EV miR-181a-5p transcriptional expression in CRC cells, forming a CCL20/CCR6/ERK1/2/Elk-1/miR-181a-5p positive feedback loop that is involved in CRLM.

3.8 | miR-181a-5p may serve as a novel biomarker for CRLM

We first performed qPCR on 30 pairs of fresh CRC tissues, and the results showed that miR-181a-5p expression was significantly higher in tissues from stage III-IV tumours compared with stage I-II tumours (Figure 8a). Then, we investigated miR-181a-5p expression in serum EVs and observed that serum EVs from CRC patients with LM exhibited higher expression levels of miR-181a-5p than those without LM (Figure 8b); representative serum EVs were examined by electron microscopy and nanoparticle tracking analysis (Figure 8c and d). Moreover, we compared miR-181a-5p expression in a TMA containing 308 CRC samples using ISH and demonstrated that the expression of miR-181a-5p in CRC tissues was notably upregulated, and it was positively correlated with TNM stage, advanced AJCC stage and tumour recurrence (Supplementary Tables S10 and S11).

To further confirm the clinical significance of miR-181a-5p expression in CRLM, we further performed IHC staining in 40 cases of fresh CRC tissues as well as in metastases to the liver to analyze the expression a CRC marker (CEA) and a fibroblast marker (α-SMA). We found that CRLM patients exhibited higher expression of miR-181a-5p, and stronger staining for CEA and α-SMA (Figure 8e; Supplementary Figure S16a). Subsequently, Kaplan-Meier survival analysis revealed that patients with higher miR-181a-5p expression had poorer DFS and OS rates (Supplementary Figure S16b and c). ISH staining and survival analysis was performed on 88 patients with CRLM that underwent simultaneous resection, and the results showed that miR-181a-5p expression was higher in these 39 patients with CRLM, and this was predictive of a poorer PFS and OS (Figure 8f and g). Furthermore, univariate and multivariate survival analyses also suggested that miR-181a-5p may serve as an independent prognostic biomarker for poor outcomes in CRLM patients (Supplementary Tables S12 and S13). Taken together, these results indicate that CRC-derived EV miR-181a-5p plays key roles in the progression of CRC, particularly in CRLM (Figure 8h).

4 | DISCUSSION

CRLM is one of the most common causes of mortality in CRC patients, and it is mediated by interactions between tumour cells and the TME in the liver. Accumulating evidence suggests that EVs are key players in intercellular communication and communication between cancer cells and the microenvironment (L. Zhang et al., 2015). miR-rich EVs have been shown to contribute to tumour metastasis in several types of cancer (Fang et al., 2018; Qin et al., 2019). In the present study, we demonstrated that highly-metastatic CRC cell-derived EVs rich in miR-181a-5p could activate HSCs by directly targeting SOCS3 via activation of the IL6/STAT3 signalling pathway, resulting in remodelling of the TME. Interestingly, activated HSCs released CCL20 which upregulated miR-181a-5p expression in CRC via the ERK/Elk-1 pathway, forming a positive feedback loop between CRC cells

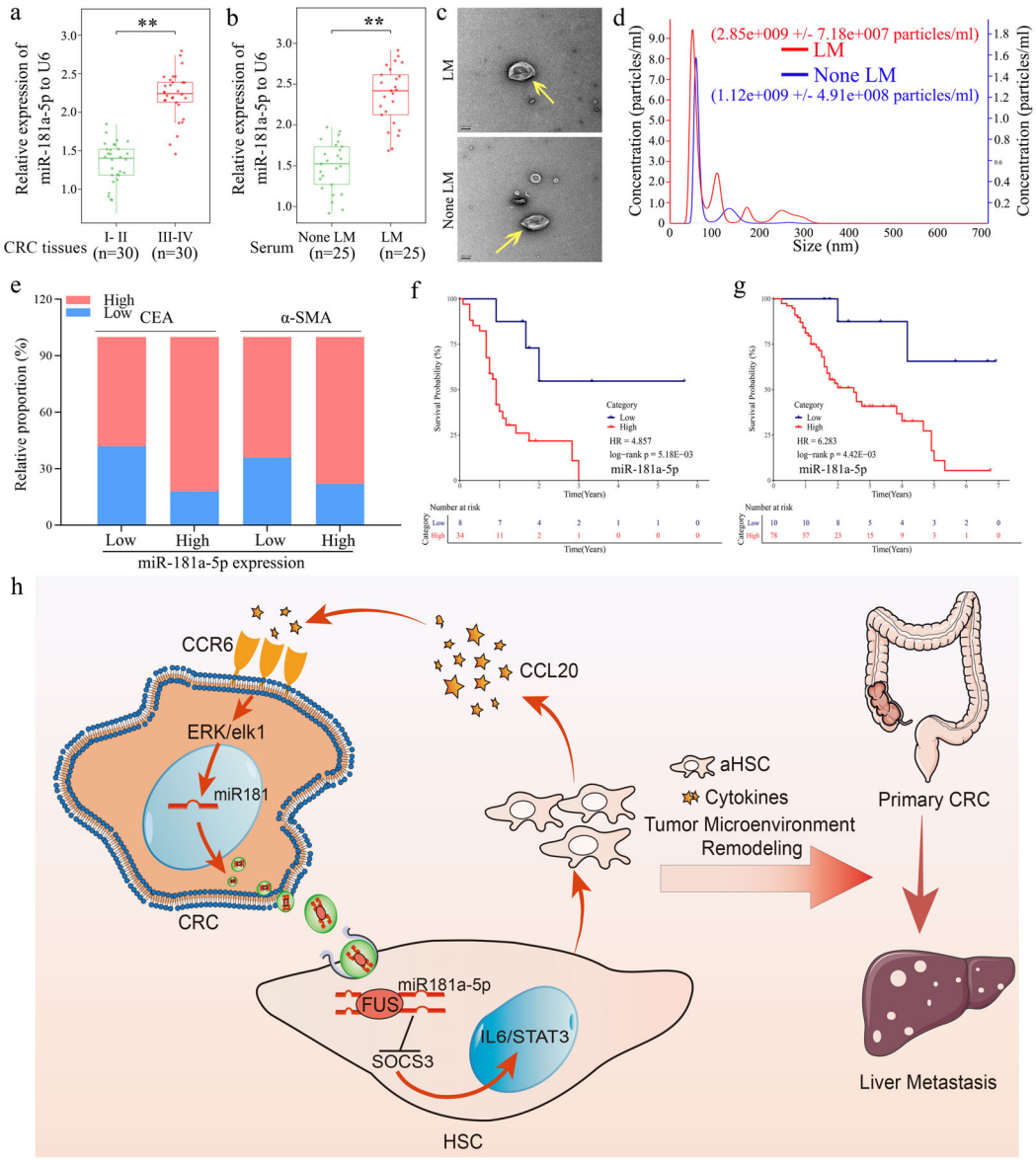

FIGURE 8 **EV miR-181a-5p serves as a novel biomarker for CRC patients with liver metastasis**. (a) The expression levels of miR-181a-5p in CRC patients with stage I-II ($n = 30$) and stage III-IV ($n = 30$) tumours were determined by qPCR. (b) qPCR assays were used to evaluate miR-181a-5p expression in serum EVs from 25 CRC patients without liver metastasis (None LM) and those with liver metastasis (LM). Serum EVs were further detected by electron microscopy (c) and Nanosight particle tracking analysis (d), respectively. Scale bar: 100 nm. (e) Association between the expression of CEA/α-SMA based on IHC staining score and miR-181a-5p in CRLM specimens. (f and g) Kaplan-Meier survival analysis and log-rank tests were used to determine the associations between miR-181a-5p with DFS (f) and OS (g) for 88 CRLM patients. (h) Schematic model of the positive feedback loop between highly metastatic CRC cells and HSCs in CRLM ($^{*}p < 0.05$; $^{**}p < 0.01$)

and HSCs, which eventually resulted in CRLM. Of note, we previously reported that ectopic expression of miR-181a-5p promoted the progression of gastric cancer (Mi et al., 2017), while other studies showed that miR-181a-5p was downregulated, and it inhibited the proliferation of CRC cells (Han et al., 2017; Lv et al., 2018), suggesting that miR-181a-5p exhibits diverse roles in different processes of cancer.

It is well established that CRLM is a multifactorial process regulated by the inherent heterogeneity and complex gene interactions that occur during cancer (Lan et al., 2019). To date, although the Kras, Braf and MMR genes have been used for predicting the prognosis of patients with metastatic CRC, they displayed efficiency in only a few cases. In addition to miR-181a-5p, other miRNAs present in EVs have also been described to alter the TME in CRC, including miR-25, miR-155 and miR-21 (Lan et al., 2019; Zeng et al., 2018). Whether with these EV miRNAs act synergistically in CRLM, and whether the impact of CRC cell-derived EV miR-181a-5p exerts a more potent effect than those of other EV miRNAs, requires further investigation.

As reported, HSCs played crucial roles in organizing and accelerating the progression of metastasis in modulating the prometastatic niche, interacting with colorectal cancer cell recruitment during CRLM development (Eveno et al., 2015).

Moreover, α-HSCs can release chemokines in response to cancer cell stimulation and liver injury, contributing to CRC invasion and growth (Chu et al., 2018; Van Den Eynden et al., 2013). Therefore, a comprehensive understanding of the underlying mechanisms involved in HSC activation and metastases to the liver may provide novel insights for therapeutic management of CRLM. In the present study, we not only confirmed that highly-metastatic CRC cell-derived EV miR-181a-5p could activate HSCs, but it was also demonstrated that α-HSCs secreted chemokine CCL20, which further activated the ERK1/2/Elk-1 signalling pathway via CCR6 in CRC cells, in-turn upregulating miR-181a-5p, resulting in reprogramming of the TME and the formation of pre-metastatic niches in CRLM. These results highlight the important roles of EV miR-181a-5p in mediating the interactions between CRC cells and the liver metastatic microenvironment. These findings may be useful in the development of novel strategies for predicting the risk of CRLM and novel treatments in the future.

In conclusion, we demonstrated that highly-metastatic CRC-derived EV miR-181a-5p activated HSCs via regulation of IL6/STAT3 signalling. This promoted secretion of CCL20 from α-HSCs and further activation of the ERK1/2/Elk-1 pathway via CCR6 and upregulation of miR-181a-5p in CRC cells, ultimately resulting in the reprogramming of the TME as well as the formation of pre-metastatic niches in liver CRLM. Our study identified a novel molecular mechanism underlying the crosstalk between CRC cells and HSCs during CRLM, and may highlight novel targets for predicting the risk of CRLM. In addition, inhibiting the feedback loop may prove to be a promising strategy for improving the prognosis of CRLM patients.

ACKNOWLEDGEMENTS

This research was supported by the National Nature Science Foundation of China (81772583, 81972293, 82003088, 81802420), Shanghai Sailing Program (19YF1409600), the Nature Science Foundation of Shandong Province (ZR2019PH008).

DATA AVAILABILITY STATEMENT

This manuscript has not been published elsewhere and is not under consideration by another journal. All authors have approved the manuscript and agree with submission to **"Journal of Extracellular Vesicles"**.

CONFLICT OF INTEREST DISCLOSURE

The authors declare that they have no conflicts of interest.

ETHICS APPROVAL STATEMENT

The study protocol conformed to the ethical guidelines of the 1975 Declaration of Helsinki and was approved by the Ethics Committee of Fudan University Shanghai Cancer Center.

PATIENT CONSENT STATEMENT

Written informed consent was obtained from each patient.

PERMISSION TO REPRODUCE MATERIAL FROM OTHER SOURCES

None.

CLINICAL TRIAL REGISTRATION

None.

GEOLOCATION INFORMATION

270 Dong'an Road, Shanghai, 200032, China.

DECLARATION OF INTEREST STATEMENT

The authors declare that they have no conflicts of interest.

REFERENCES

Affo, S., Yu, L.-X, & Schwabe, R. F.. (2017). The role of cancer-associated fibroblasts and fibrosis in liver cancer. *Annual Review of Pathology*. *12*, 153–186.

Ahmad, S. A., Berman, R. S., & Ellis, L. M.. (2003). Biology of colorectal liver metastases. *Surgical Oncology Clinics of North America*. *12*, 135-150.

Beckers, R. C. J., Lambregts, D. M. J., Lahaye, M. J., Rao, S. -. X., Kleinen, K., Grootscholten, C., Beets, G. L., Beets-Tan, R. G. H., & Maas, M.. (2018). Advanced imaging to predict response to chemotherapy in colorectal liver metastases—A systematic review. *HPB (Oxford)*. *20*, 120–127.

Brenner, C., Galluzzi, L., Kepp, O., & Kroemer, G.. (2013). Decoding cell death signals in liver inflammation. *Journal of Hepatology*. *59*, 583-594.

Chu, X., Jin, Q., Chen, H., Wood, G. C., Petrick, A., Strodel, W., Gabrielsen, J., Benotti, P., Mirshahi, T., Carey, D. J., Still, C. D., Distefano, J. K., & Gerhard, G. S. (2018). CCL20 is up-regulated in non-alcoholic fatty liver disease fibrosis and is produced by hepatic stellate cells in response to fatty acid loading. *Journal of Translational Medicine*. *16*, 108.

Conde-Vancells, J., Rodriguez-Suarez, E., Embade, N., Gil, D., Matthiesen, R., Valle, M., Elortza, F., Lu, S. C., Mato, J. M., & Falcon-Perez, J. M.. (2008). Characterization and comprehensive proteome profiling of exosomes secreted by hepatocytes. *Journal of Proteome Research*. *7*, 5157-5166.

Cook, K. B., Kazan, H., Zuberi, K., Morris, Q., & Hughes, T. R.. (2011). RBPDB: A database of RNA-binding specificities. *Nucleic Acids Research*. *39*, D301-D308.

Eveno, C., Hainaud, P., Rampanou, A., Bonnin, P., Bakhouche, S., Dupuy, E., Contreres, J. -. O., & Pocard, M.. (2015). Proof of prometastatic niche induction by hepatic stellate cells. *Journal of Surgical Research*. *194*, 496–504.

Fang, T., Lv, H., Lv, G., Li, T., Wang, C., Han, Q., Yu, L., Su, Bo, Guo, L., Huang, S., Cao, D., Tang, L., Tang, S., Wu, M., Yang, W., & Wang, H. (2018). Tumor-derived exosomal miR-1247-3p induces cancer-associated fibroblast activation to foster lung metastasis of liver cancer. *Nature Communications*. *9*, 191.

Han, P., Li, J. -. W., Zhang, Bo-M, Lv, J. -. C., Li, Y. -. M., Gu, X. -. Y., Yu, Z. -. W., Jia, Y-He, Bai, X. -. F., Li, Li, Liu, Y. -. L., & Cui, B. -. B. (2017). The lncRNA CRNDE promotes colorectal cancer cell proliferation and chemoresistance via miR-181a-5p-mediated regulation of Wnt/beta-catenin signaling. *Molecular Cancer*. *16*, 9.

Illemann, M., Eefsen, R. H. L., Bird, N. C., Majeed, A., Osterlind, K., Laerum, O. D., Alpízar-Alpízar, W., Lund, I. K., & Høyer-Hansen, G.. (2016). Tissue inhibitor of matrix metalloproteinase-1 expression in colorectal cancer liver metastases is associated with vascular structures. *Molecular Carcinogenesis*. *55*, 193–208.

Kadomoto, S., Izumi, K., & Mizokami, A.. (2020). The CCL20-CCR6 axis in cancer progression. *International Journal of Molecular Sciences*. *21*, 5186.

Lan, J., Sun, L., Xu, F., Liu, L., Hu, F., Song, D., Hou, Z., Wu, W., Luo, X., Wang, J., Yuan, X., Hu, J., & Wang, G. (2019). M2 Macrophage-Derived Exosomes Promote Cell Migration and Invasion in Colon Cancer. *Cancer Res*. *79*, 146-158.

Lesina, M., Kurkowski, M. U., Ludes, K., Rose-John, S., Treiber, M., Klöppel, G., Yoshimura, A., Reindl, W., Sipos, B., Akira, S., Schmid, R. M., & Algül, H. (2011). Stat3/Socs3 activation by IL-6 transsignaling promotes progression of pancreatic intraepithelial neoplasia and development of pancreatic cancer. *Cancer Cell*. *19*, 456-469.

Li, H., Chehade, M., Liu, W., Xiong, H., Mayer, L., & Berin, M. C.. (2007). Allergen-IgE complexes trigger CD23-dependent CCL20 release from human intestinal epithelial cells. *Gastroenterology*. *133*, 1905-1915.

Lv, S. -. Y., Shan, Ti-D, Pan, X. -. T., Tian, Zi-B, Liu, Xi-S, Liu, Fu-G, Sun, X. -. G., Xue, H. -. G., Li, X. -. H., Han, Y., Sun, Li-J, Chen, Li, & Zhang, L. -. Y. (2018). The lncRNA ZEB1-AS1 sponges miR-181a-5p to promote colorectal cancer cell proliferation by regulating Wnt/beta-catenin signaling. *Cell Cycle*. *17*, 1245–1254.

Mi, Y., Zhang, D., Jiang, W., Weng, J., Zhou, C., Huang, K., Tang, H., Yu, Y., Liu, X., Cui, W., Zhang, M., Sun, X., Zhou, Z., Peng, Z., Zhao, S., & Wen, Y. (2017). miR-181a-5p promotes the progression of gastric cancer via RASSF6-mediated MAPK signalling activation. *Cancer Letters*. *389*, 11–22.

Olaso, E., Santisteban, A., Bidaurrazaga, J., Gressner, A. M., Rosenbaum, J., & Vidal-Vanaclocha, F.. (1997). Tumor-dependent activation of rodent hepatic stellate cells during experimental melanoma metastasis. *Hepatology*. *26*, 634-642.

Qin, X., Guo, H., Wang, X., Zhu, X., Yan, M., Wang, Xu, Xu, Q., Shi, J., Lu, E., Chen, W., & Zhang, J. (2019). Exosomal miR-196a derived from cancer-associated fibroblasts confers cisplatin resistance in head and neck cancer through targeting CDKN1B and ING5. *Genome Biology*. *20*, 12.

Rokavec, M., Öner, M. G., Li, H., Jackstadt, R., Jiang, L., Lodygin, D., Kaller, M., Horst, D., Ziegler, P. K., Schwitalla, S., Slotta-Huspenina, J., Bader, F. G., Greten, F. R., & Hermeking, H. (2014). IL-6R/STAT3/miR-34a feedback loop promotes EMT-mediated colorectal cancer invasion and metastasis. *Journal of Clinical Investigation*. *124*, 1853-1867.

Schütte, M., Risch, T., Abdavi-Azar, N., Boehnke, K., Schumacher, D., Keil, M., Yildiriman, R., Jandrasits, C., Borodina, T., Amstislavskiy, V., Worth, C. L., Schweiger, C., Liebs, S., Lange, M., Warnatz, H. -. J., Butcher, L. M., Barrett, J. E., Sultan, M., Wierling, C., Golob-Schwarzl, N., … Yaspo, M. -. L.. (2017). Molecular dissection of colorectal cancer in pre-clinical models identifies biomarkers predicting sensitivity to EGFR inhibitors. *Nature Communications*. *8*, 14262.

Van Den Eynden, G. G., Majeed, A. W., Illemann, M., Vermeulen, P. B., Bird, N. C., Høyer-Hansen, G., Eefsen, R. L., Reynolds, A. R., & Brodt, P.. (2013). The multifaceted role of the microenvironment in liver metastasis: Biology and clinical implications. *Cancer Research*. *73*, 2031-2043.

Wei, P., Wu, F., Kang, B., Sun, X., Heskia, F., Pachot, A., Liang, Ji, & Li, D.. (2020). Plasma extracellular vesicles detected by Single Molecule array technology as a liquid biopsy for colorectal cancer. *Journal of Extracellular Vesicles*. *9*, 1809765.

Yasukawa, H., Ohishi, M., Mori, H., Murakami, M., Chinen, T., Aki, D., Hanada, T., Takeda, K., Akira, S., Hoshijima, M., Hirano, T., Chien, K. R., & Yoshimura, A. (2003). IL-6 induces an anti-inflammatory response in the absence of SOCS3 in macrophages. *Nature Immunology*. *4*, 551-556.

Zeng, Z., Li, Y., Pan, Y., Lan, X., Song, F., Sun, J., Zhou, K., Liu, X., Ren, X., Wang, F., Hu, J., Zhu, X., Yang, W., Liao, W., Li, G., Ding, Y., & Liang, L. (2018). Cancer-derived exosomal miR-25-3p promotes pre-metastatic niche formation by inducing vascular permeability and angiogenesis. *Nat Commun*. *9*, 5395.

Zhang, D. Y., Goossens, N., Guo, J., Tsai, M. -. C., Chou, H. -. I., Altunkaynak, C., Sangiovanni, A., Iavarone, M., Colombo, M., Kobayashi, M., Kumada, H., Villanueva, A., Llovet, J. M., Hoshida, Y., & Friedman, S. L. (2016). A hepatic stellate cell gene expression signature associated with outcomes in hepatitis C cirrhosis and hepatocellular carcinoma after curative resection. *Gut*. *65*, 1754-1764.

Zhang, L., Zhang, S., Yao, J., Lowery, F. J., Zhang, Q., Huang, W. -. C., Li, P., Li, M., Wang, X., Zhang, C., Wang, H., Ellis, K., Cheerathodi, M., Mccarty, J. H., Palmieri, D., Saunus, J., Lakhani, S., Huang, S., Sahin, A. A., Aldape, K. D., Steeg, P. S., & Yu, D. (2015). Microenvironment-induced PTEN loss by exosomal microRNA primes brain metastasis outgrowth. *Nature*. *527*, 100–104.

Zhao, S., Guan, B., Mi, Y., Shi, D., Wei, P., Gu, Y., Cai, S., Xu, Ye, Li, X., Yan, D., Huang, M., & Li, D. (2021). LncRNA MIR17HG promotes colorectal cancer liver metastasis by mediating a glycolysis-associated positive feedback circuit. *Oncogene*. *40*, 4709-4724.

Zhao, S., Mi, Y., Guan, B., Zheng, B., Wei, P., Gu, Y., Zhang, Z., Cai, S., Xu, Ye, Li, X., He, X., Zhong, X., Li, G., Chen, Z., & Li, D. (2020). Tumor-derived exosomal miR-934 induces macrophage M2 polarization to promote liver metastasis of colorectal cancer. *Journal of Hematology & Oncology*. *13*, 156.

Zhao, S., Sun, H., Jiang, W., Mi, Y., Zhang, D., Wen, Y., Cheng, D., Tang, H., Wu, S., Yu, Y., Liu, X., Cui, W., Zhang, M., Sun, X., Zhou, Z., Peng, Z., & Yan, D. (2017). miR-4775 promotes colorectal cancer invasion and metastasis via the Smad7/TGFbeta-mediated epithelial to mesenchymal transition. *Molecular Cancer*. *16*, 12.

SUPPORTING INFORMATION

Additional supporting information may be found in the online version of the article at the publisher's website.

How to cite this article: Zhao, S., Mi, Y., Zheng, B., Wei, P., Gu, Y., Zhang, Z., Xu, Y., Cai, S., Li, X., & Li, D. (2022). Highly-metastatic colorectal cancer cell released miR-181a-5p-rich extracellular vesicles promote liver metastasis by activating hepatic stellate cells and remodeling the tumor microenvironment. *Journal of Extracellular Vesicles*, *11,* e12186. https://doi.org/10.1002/jev2.12186